4.5 Å (d_{001}(calc) = 8.12 Å) for the parallel disposition of the binuclear core in the layers, which is 1.7 Å greater than the observed d-spacing.

A transverse arrangement of the Mo_2^{5+} core permits interlayer keying of the host with the guest structure. This guest-host interaction, which has been observed by us previously in the ion-exchange chemistry of *trans*-dioxorhenium(V) complexes in layered oxides,[47] may provide a clue to the anomalous magnetic behavior of the Mo_2^{5+} intercalate. The observed enhancement in spin-spin coupling may result from increased interlayer communication owing to the smaller d-spacing of the Mo_2^{5+} intercalate (d_{001} = 6.4 Å) as compared to the Na^+-intercalated (d_{001} = 6.7 Å) species. However, the EPR experiments show that the spin interactions within the layers are obviously modulated by the physical linkage of a magnetically active $S = {}^1/_2$ guest. The arrangement of spin ${}^1/_2$ guests keyed into the two-dimensional magnetic layer should give rise to an anisotropic magnetic exchange interaction, thereby modifying the magnetic behavior of the layers. Indeed, the observance of unusual magnetism upon the synthesis of two-dimensional magnetic host layers intercalated with a magnetic guest has precedent. Clement et al. have described spontaneous magnetization below ~90 K for layered $FePS_3$ intercalated with pyridinium.[95] Our results coupled with those of Clement suggest that the ability to synthesize lamellar solids with anisotropically arranged magnetic guests may lead to interesting magnetically-ordered systems.

Thus layered metal phosphate are ideal host structures for $M\overset{4}{-}M$ guests. The physical and chemical properties of LMPs are compatible with those properties of $M\overset{4}{-}M$ cores, and indeed the coordination environments of $M\overset{4}{-}M$ centers in molecular solids can be achieved within the gallery regions of LMPs. In the context of designing photoactive $M\overset{4}{-}M$—LMP intercalates, investigations of tetrakis(phosphato)dimolybdenum have shown their photoredox chemistry to be restricted to one-electron transformations owing to the inability of the rigid phosphate coordination sphere to stabilize high oxidation states of the metal core.[46] Conversely, multielectron phototransformations are promoted at $M\overset{4}{-}M$ cores when coordinated by ligands that can stabilize metals in high formal oxidation states. One such class of complexes is the $M_2X_4(\overset{\frown}{LL})_2$ species, where $\overset{\frown}{LL}$ is a bidentate phosphine or hydroxypyridine. Upon excitation, rearrangement of the halide ligands to yield bioctahedral geometries promotes the two-electron photooxidations of these $M\overset{4}{-}M$ species.[46] To this end, studies are underway to introduce $M\overset{4}{-}M$ cores into LMP galleries that are modified with $\overset{\frown}{LL}$ functionality.

Acknowledgment. We thank Matt Espe for assistance in obtaining low-temperature EPR. Financial support from the National Science Foundation (CHE-9100532) and the Center for Fundamental Materials Research is gratefully acknowledged.

Supplementary Material Available: A table listing the observed and calculated peak positions and the indices of powder X-ray diffraction patterns of layered metal phosphates, ESCA spectra of $NbOPO_4 \cdot 3H_2O$, Na^+-intercalated $NbOPO_4$ host layers and of the solids obtained from the reaction of $[Mo_2(CH_3CN)_8](BF_4)_4$ with $NbOPO_4 \cdot 3H_2O$ and Na^+-intercalated $NbOPO_4$, and powder X-ray diffraction patterns of $NbOPO_4 \cdot 3H_2O$, Na^+-intercalated $VOPO_4$ host layers and of the solids obtained from the reaction of $[Mo_2(CH_3CN)_8](BF_4)_4$ with $NbOPO_4 \cdot 3H_2O$ and Na^+-intercalated $NbOPO_4$ (4 pages). Ordering information is given on any current masthead page.

(95) Clement, R.; Lomas, L.; Audiere, J. P. *Chem. Mater.* **1990**, *2*, 641.

Generation of Au^{2+} Ions in the Solid State or in Fluorosulfuric Acid Solution and Their Identification by ESR

F. G. Herring,* G. Hwang, K. C. Lee, F. Mistry, P. S. Phillips, H. Willner,† and F. Aubke*

Contribution from the Department of Chemistry, The University of British Columbia, 2036 Main Mall, Vancouver, British Columbia, Canada V6T 1Y6. *Received June 14, 1991*

Abstract: The partial pyrolysis of gold(III) fluorosulfate, $Au(SO_3F)_3$, at temperatures below 145 °C allows the generation of Au^{2+} defects in the solid residue by reductive elimination of $SO_3F^\bullet$ radicals. Solvated Au^{2+} is obtained by the reduction of $Au(SO_3F)_3$ in HSO_3F solution by gold powder at 65 °C. Both systems are studied by ESR and identical high g_{iso} values of g = 2.360 are found. Hyperfine splitting due to ^{197}Au, $I = 3/2$, is observed in frozen solutions of Au^{2+}(solv). Pyrolysis of $Br_3[Au(SO_3F)_4]$ also gives partly pyrolyzed $Au(SO_3F)_3$, with a sufficiently high Au^{2+} ion concentration, to allow a magnetic susceptibility study between 100 and 295 K.

Introduction

Compounds or complexes with gold in the oxidation state +2 are rather uncommon.[1,2] Previously reported examples of isolated compounds may be grouped into three general categories.

(a) *Polynuclear* Au(I)/Au(III) compounds comprise the first category, with gold(II) chloride, Au_4Cl_8,[3] a typical example. As expected, gold(I) exhibits linear, and gold(III) square-planar coordination. The existence of this group, termed "pseudogold(II)" compounds,[2] reflects the tendency of gold(II), $5d^9$, to disproportionate completely into gold(I), $5d^{10}$, and gold(III), $5d^8$.

† Permanent address: Institut für Anorganische Chemie, der Universität, Callinstrasse 9, D Hannover.

(1) (a) Puddephatt, R. J. *The Chemistry of Gold*; Elsevier: Amsterdam, The Netherlands, 1978. (b) Puddephatt, R. J. In *Comprehensive Coordination Chemistry*; Wilkinson, G., Ed.; Pergamon Press: Oxford, U.K., 1987; Vol. 7, p 861.

(2) Schmidbaur, H.; Dash, K. C. *Adv. Inorg. Chem. Radiochem.* **1982**, *25*, 39.

(3) (a) Dell'Amico, D. B.; Calderazzo, F.; Marchetti, F.; Merlino, S.; Perego, G. *J. Chem. Soc., Chem. Commun.* **1977**, 31. (b) Dell'Amico, D. B.; Calderazzo, F.; Marchetti, F.; Merlino, S. *J. Chem. Soc. Dalton Trans.* **1982**, 2257.

0002-7863/92/1514-1271$03.00/0

(b) *Binuclear* gold(II) compounds with a gold–gold bond, e.g., in $Au_2I_2[\mu\text{-}(CH_2)_2P(CH_3)_2]_2$[1,2,4] and related compounds, comprise the second category.

(c) *Mononuclear*, anionic gold(II) complexes formed with a variety of polydentate, anionic ligands such as chelating dithiolates, as in $[Au(1,2\text{-}S_2C_2(CN)_2)_2]^{2-}$, $[Au(mnt)_2]^{2-}$,[5] π-bonding 1,2-dicarbollides as in $[Au(C_2B_9H_{11})_2]^{2-}$,[6] or phthalocyanine, resulting in a neutral complex,[7] represent the third category. Examples in this group are paramagnetic, while those in groups (a) and (b) are diamagnetic, as expected. However, magnetic moments are reported for examples from group (c) in only two instances and at room temperature only as 1.79[6] and 1.87 μ_B,[7] respectively. Detailed electron spin resonance (ESR) studies, which are much more abundant,[1,2,5,7-9] strongly suggest that the unpaired electron resides predominantly on the ligands, as estimated from the coupling to the 3/2 nuclear spin of ^{197}Au, which roughly corresponds to 15% spin density at the gold center.

In summary, it appears that mononuclear, paramagnetic Au(II) complexes are formed where good σ-donor and π-acceptor ligands stabilize the metal center. The oxidation state of gold in these complexes is, however, obscured by extensive delocalization of the unpaired electron toward the ligand. The radical anion $[AuCl_4]^{2-\bullet}$ may be considered an exception. This species is postulated, based on kinetic evidence only, as a reactive intermediate in the reduction of $[AuCl_4]^-$ by aqueous Fe^{2+} ions.[10]

We wish to report here on two methods to generate paramagnetic Au^{2+} ions, stabilized either by weakly basic SO_3F ligands or in strongly acidic HSO_3F: (i) the partial thermal decomposition of solid gold(III) fluorosulfate, $Au(SO_3F)_3$, and some of its derivatives,[11,12] which proceeds via reductive elimination of $SO_3F^\bullet$ radicals[13] and the concomitant formation of Au^{2+} defects in the solid residue, and (ii) the reduction of $Au(SO_3F)_3$, dissolved in fluorosulfuric acid, with gold powder, which produces solvated Au^{2+} cations.

Both species are studied by ESR. Magnetic susceptibility measurements on the solid are obtained between 298 and 100 K. The ESR spectra obtained on frozen solutions or solids are similar for both samples but differ substantially from those reported previously[1,2,5,7-9] for mononuclear gold(II) complexes.

Experimental Section

(a) Chemicals. Gold powder, −20 mesh of 99.95% purity was obtained from the Ventron Corporation (Alfa Inorganics). Literature methods were employed to synthesize bis(fluorosulfuryl)peroxide, $S_2O_6F_2$,[14] bromine(I) fluorosulfate,[15] gold(III) fluorosulfate,[12] $Cs[Au(SO_3F)_4]$,[12] and cesium fluorosulfate[16] and to purify technical grade fluorosulfuric acid (Orange County Chemicals).[16]

(b) Instrumentation. Infrared spectra were recorded on a Perkin-Elmer 598 grating spectrometer. Solid samples were pressed as thin films between KBr, AgCl, or AgBr windows (Harshaw Chemicals). Gaseous samples were studied in Pyrex or Monel cells of 10-cm path length, fitted with silver bromide windows. Magnetic susceptibilities were measured using the Gouy apparatus described earlier.[17] The magnet's coil current was regulated to give a field of approximately 4500 G. The sample temperature was controlled by the evaporation rate of N_2 around the chamber. Calibration was achieved using $HgCo(SCN)_4$.[18] Diamagnetic corrections of -27×10^{-6} cm^3 mol^{-1} for Au^{3+} and -40×10^{-6} cm^3 mol^{-1} for SO_3F^- were employed.[9]

Solid samples were manipulated inside a Vacuum Atmosphere Corp. Dri-Lab, Model HE-493, filled with dry N_2, and equipped with a HE-493 Dri-Train. Standard vacuum line techniques were employed for the manipulation of volatile compounds. A Setra (Setra Systems Inc. Action, MA) pressure transducer Model 280E was used as a pressure gauge. Some of the reactions were performed in sealed-off, all-glass ampoules. The ampoule was opened in vacuo, using an "ampoule key" as described previously.[19] Pyrex reaction vials of 120-mm length and 10-mm o.d. or round-bottom flasks fitted with Young valves were used on occasion. An apparatus as described by Shriver[20] was used for the filtration of the moisture-sensitive reaction mixture. Chemical analyses were performed by Mr. P. Borda of this department.

ESR Instrumentation. The samples were held at 103 K using a Varian E-257 temperature controller, and the ESR spectra were run on an X-band homodyne spectrometer with a Varian 12-in. magnet equipped with a MkII field-dial control. An Ithaco Dynatrac 391A lock-in amplifier was used to obtain phase-sensitive detection at 100 kHz. Data acquisition was carried out using a Qua-Tech 12-bit data-acquisition board (ADM 12-10), together with a Qua-Tech parallel expansion board (PXB-721) incorporated into an IBM XT computer. The relevant data-processing software was as described previously.[21-23] The microwave frequency was measured with a HP5246L frequency counter equipped with a HP5255A plug-in. Field calibration was accomplished using a Varian Gaussmeter, the output of which was also collected by the IBM computer. The absolute field was corrected for the placement of the gaussmeter probe by calibrating against peroxylamine sulfate in aqueous solution and was in error by ca. 0.01 G. The precision of the data is typically ca. 0.02 G for 2 K points over a 100-G sweep which, together with the ca. 10-kHz error in the microwave frequency, corresponds to an error of ca. 0.000 02 in the g values quoted.

ESR Simulations. The spin Hamiltonian parameters for the observed centers were determined using the equation

$$\mathcal{H} = \beta \mathbf{B}\cdot\mathbf{g}\cdot\mathbf{S} + \mathbf{S}\cdot A\cdot\mathbf{I} + Q_{zz}[\mathbf{E}\mathbf{I}_z^2 - \mathbf{I}(\mathbf{I}+1)] + \mathbf{Q}_{xy}[\mathbf{I}_x^2 - \mathbf{I}_y^2]$$

implemented in a program that diagonalizes the total matrix. The program is called QPOW and was obtained from the Illinois ESR Research Center (NIH resources Grant No. RR01811) and was used on a 386 PC. The principal values of the g tensor, and the A and Q tensors when necessary, were obtained by matching the observed and simulated spectra computed for polycrystalline samples. The goodness of the fit was established by computer subtraction of the observed and simulated spectra in digital form to obtain a linear residual to within 2% of the total spectrum.

(c) Synthetic Procedures. (i) The Preparation of $Au(SO_3F)_3$ for a Magnetic Susceptibility Measurement. Gold powder (0.390 g) was warmed up with an excess of $BrSO_3F$ from a $CHClCCl_2$ slush bath (−60 °C) overnight. This precaution was taken because it was found that if the reactants were warmed up quickly, a violent reaction would occur, causing the $BrSO_3F$ to reflux in the vessel. The gold powder completely dissolved into a thick dark brown liquid that was then heated to 70 °C for 1 day to ensure complete oxidation. After removing the volatile products and unreacted $BrSO_3F$, a light brown crystalline solid was obtained (1.627 g, calcd $Br_3[Au(SO_3F)_4]$, 1.649 g). The material melted without decomposition at 76–80 °C in 1 atm of N_2 to a viscous, dark brown liquid. The compound was diamagnetic, with $X_M = -246 \times 10^{-6}$ cm^3 mol^{-1} at 291 K, and was found to attack AgCl windows.

When the solid product was heated in vacuo at over 60 °C, it began to lose weight. Typically a sample (2.470 g) heated for 1 day yielded bright orange crystals, 1.428 g, corresponding to $Au(SO_3F)_3$ (calcd 1.433 g). The low temperature was necessary to prevent melting of the adduct or sublimation (at about 80 °C). The sample obtained was weakly paramagnetic, as discussed below.

(ii) Pyrolysis of $Au(SO_3F)_3$. A 100-mL, round-bottom flask containing 265 mg of $Au(SO_3F)_3$ (0.536 mmol) was heated in a 60 °C oil bath for 7 days. No sublimate or change in color of the compound was observed. There were no measurable volatiles when the sample was cooled to −196 °C throughout the pyrolysis. At room temperature, 9.8

(4) Fackler, J. P.; Basil, J. D. In *Inorganic Chemistry toward the 21st Century*; Chisholm, M. H., Ed.; ACS Symposium Series, 211; American Chemical Society: Washington, DC, 1983; p 201. *Organometallics* **1982**, *1*, 871.
(5) Schlupp, R. L.; Maki, A. H. *Inorg. Chem.* **1974**, *13*, 44.
(6) Warren, L. F.; Hawthorne, M. F. *J. Am. Chem. Soc.* **1968**, *90*, 4823.
(7) (a) MacCragh, A.; Koski, W. S. *J. Am. Chem. Soc.* **1963**, *85*, 2375. (b) MacCragh, A.; Koski, W. S. *J. Am. Chem. Soc.* **1965**, *87*, 2496.
(8) Waters, J. H.; Gray, H. B. *J. Am. Chem. Soc.* **1965**, *87*, 3534.
(9) Landolt-Börnstein. Numerical Data and Functional Relationships in Science and Technology. Vol. 2. *Magnetic Properties of Coordination and Organometallic Transition Metal Compounds*; Springer Verlag: Berlin, 1966.
(10) Rich, R. L.; Taube, H. *J. Phys. Chem.* **1954**, *58*, 6.
(11) Johnson, W. M.; Dev, R.; Cady, G. H. *Inorg. Chem.* **1972**, *11*, 2260.
(12) (a) Lee, K. C.; Aubke, F. *Inorg. Chem.* **1979**, *18*, 389. (b) Lee, K. C.; Aubke, F. *Inorg. Chem.* **1980**, *19*, 119.
(13) Dudley, F. B.; Cady, G. H. *J. Am. Chem. Soc.* **1963**, *85*, 3375.
(14) (a) Dudley, F. B.; Cady, G. H. *J. Am. Chem. Soc.* **1957**, *79*, 513. (b) Cady, G. H.; Shreeve, J. M. *Inorg. Synth.* **1963**, *7*, 124.
(15) Aubke, F.; Gillespie, R. J. *Inorg. Chem.* **1968**, *7*, 599.
(16) Barr, J.; Gillespie, R. J.; Thompson, R. C. *Inorg. Chem.* **1964**, *3*, 1149.
(17) Clark, H. C.; O'Brien, R. J. *Can. J. Chem.* **1961**, *39*, 1030.
(18) Figgis, B. N.; Nyholm, R. S. *J. Chem. Soc.* **1958**, 4190.
(19) Gombler, W.; Willner, H. *J. Phys. E. Sci. Instrum.* **1987**, *20*, 1286.
(20) Shriver, D. R. *The Manipulation of Air-Sensitive Compounds*; McGraw-Hill: New York, NY, 1969.
(21) Herring, F. G.; Phillips, P. S. *J. Magn. Reson.* **1984**, *57*, 43.
(22) Herring, F. G.; Phillips, P. S. *J. Magn. Reson.* **1985**, *62*, 19.
(23) McLung, R. E. D. *Can. J. Phys.* **1968**, *46*, 2271.

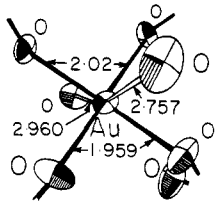

Figure 1. The coordination environment of Au(III) in $[Au(SO_3F)_3]_2$. Interatomic distances are quoted in Å: ref 24.

μmol volatiles were obtained and removed in vacuo. The oil-bath temperature was increased to 100 °C, and the flask was heated for ~4 days. An orange sublimate appeared on the walls of the reactor. Seven μmol volatiles were measured at room temperature and removed in vacuo. The oil-bath temperature was increased to 125 °C. The $Au(SO_3F)_3$ was heated for ≈2 days, and 5.8 μmol volatiles were measured and again removed in vacuo. The sublimate was scraped from the walls of the reactor, and the compound returned to the oil bath for 7 days. The overall observed weight loss of the $Au(SO_3F)_3$ was 17.8 mg or 0.036 mmol. The melting range of partly pyrolyzed $Au(SO_3F)_3$ was 138–139 °C (lit. 140 °C[7]). The sulfur content of the sample was 18.9% vs a calculated value of 19.47%.

(iii) Reduction of Au(III) to Au(II). The reduction of $Au(SO_3F)_3$ by gold powder was carried out at 65 °C. Approximately 3 mL of HSO_3F was added to a mixture of $Au(SO_3F)_3$ (255 mg, 0.516 mmol) and gold metal (42 mg, 0.213 mmol) and stirred at room temperature. The solids dissolved to give a solution that was initially opaque and orange. After about 15 min, the color darkened to orange-red. Over a period of about 4 h, the turbid, dark orange-red solution gradually became clear. After heating overnight at 65 °C in an oil bath, the gold metal had completely dissolved, and the stirred solution had a dark orange-brown color. After 3 days a yellow-orange solid started to form. This material was isolated by vacuum filtration and analyzed as $Au(SO_3F)_2$. The solution color remained unchanged. An ESR spectrum of the solution was recorded. No ESR signal was obtainable from the solid.

Results and Discussion

Three relevant aspects are addressed in this study: (i) initial experimental evidence for Au^{2+} obtained from magnetic susceptibility measurements between 298 and 100 K, (ii) the generation of Au^{2+} ions in the solid state and in fluorosulfuric acid solution, and (iii) the identification of Au^{2+} by ESR spectroscopy.

Gold(III) fluorosulfate, $Au(SO_3F)_3$, is found to be the key compound in this investigation, and some puzzling observations made during its synthesis mark the starting point. The original synthesis of $Au(SO_3F)_3$, from gold powder and an excess of bromine(I) fluorosulfate, $BrSO_3F$,[11] proceeds through a solid intermediate, subsequently[12b] identified as $Br_3[Au(SO_3F)_4]$. This intermediate is diamagnetic; however, pyrolyses at elevated temperatures afford weakly paramagnetic $Au(SO_3F)_3$ with $\mu_{eff}^{295} = 0.54$ μ_B.

An alternate, more direct route, the oxidation of gold powder by bis(fluorosulfuryl)peroxide, $S_2O_6F_2$, in HSO_3F as solvent, results in diamagnetic $Au(SO_3F)_3$ ($\chi_M = -146 \times 10^{-6}$ cm^3 mol^{-1}), isolated at room temperature. Diamagnetism, expected for gold(III) compounds,[1,2,9] is consistent with the dimeric molecular structure,[24] and the coordination environment of gold (Figure 1) shows the metal in a slightly distorted, square-planar environment, with intermolecular contacts completing a strongly distorted octahedral coordination geometry.

There are several alternative explanations for the weak paramagnetism in some samples of $Au(SO_3F)_3$; however, they must be ruled out on experimental grounds: (i) The occurrence of temperature-independent paramagnetism (TIP) in some samples but not in others is unlikely, since the Curie–Weiss law is followed between 295 and 100 K (Figure 2). The observation of TIP in one sample but not in another would imply two different structural forms of gold(III) fluorosulfate. (ii) Pyrolysis of the Br_3^+ cation in $Br_3[Au(SO_3F)_4]$ could conceivably result in the formation of the dibromine cation Br_2^+. This cation, found so far only in $Br_2^+[Sb_3F_{16}^-]$[25] or in superacid solution,[26] has a $^2\pi_{3/2}$ ground state

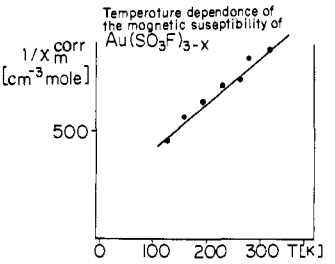

Figure 2. The temperature dependence of the magnetic susceptibility of $Au(SO_3F)_3$, obtained by pyrolysis of $Br_3[Au(SO_3F)_4]$ between 100 and 295 K.

and the magnetic susceptibility follows Curie–Weiss law,[27,28] but samples of $Au(SO_3F)_3$ obtained via $Br_3[Au(SO_3F)_4]$ do not contain bromine.[11]

A remaining plausible explanation for the observed magnetic behavior is the presence of Au^{2+} as a lattice defect in solid $Au(SO_3F)_3$[29] [Curie–Weiss law behavior is also found for Ag^{2+} in $Ag(SO_3F)_2$,[29] and only at very low temperatures (~40 K) is ferromagnetic coupling observed.[30]] Interestingly, $Ag(SO_3F)_2$ on heating to 215 °C undergoes reductive elimination of $SO_3F^\bullet$ radicals, to give quantitatively silver(I) fluorosulfate.[29]

Another relevant example for this decomposition mode of a metal fluorosulfate is found in the mixed-valence compound $Pd^{II}Pd^{IV}(SO_3F)_6$, which decomposes at 160 °C to $Pd(SO_3F)_2$ and $S_2O_6F_2$.[31] The reported decomposition of $Xe(SO_3F)_2$ to Xe and $S_2O_6F_2$ at 45 °C[32] provides the only other example for the reductive elimination of fluorosulfate radicals, which then recombine to form $S_2O_6F_2$. Reductive elimination of bromine(I) fluorosulfate is observed[33] when $Cs_2[Pd(SO_3F)_6]$ is reduced by Br_2 to give $Cs_2[Pd(SO_3F)_4]$. It is hence likely that reductive elimination of $BrSO_3F$ and, perhaps initially, $SO_3F^\bullet$ radicals occurs during the pyrolysis of $Br_3[Au(SO_3F)_4]$, leading to a residue of the composition $Au(SO_3F)_n$, with $n < 3$.

It is noteworthy that a similar situation to the one suggested for $Au(SO_3F)_3$ is reported for gold(III) fluoride. A sample obtained by fluorination of gold with F_2 is diamagnetic,[34] while fluorination with bromine(III) fluoride and pyrolysis of the intermediate $BrF_2[AuF_4]$ at 180 °C[35] produces weakly paramagnetic AuF_3 with $\mu_{eff}^{295} = 0.5$ μ_B.[36]

In summary, the magnetic behavior of the residue and the relevant precedents cited suggest the formation of some Au^{2+} during pyrolysis. Identification and characterization of Au^{2+} using ESR spectroscopy will be discussed below. For the preparation of suitable samples for ESR measurements, the controlled pyrolysis of $Au(SO_3F)_3$ in a closed, evacuated reactor is chosen over pyrolysis of $Br_3[Au(SO_3F)_4]$ for the following reasons.

(i) A straightforward course of the pyrolysis reaction is expected, with elimination of $SO_3F^\bullet$ radicals or the dimer $S_2O_6F_2$ anticipated. The reaction is easily monitored by measuring the pressure increase in the closed system and the weight loss after removal of all volatile products.

(ii) The molecular structure of $Au(SO_3F)_3$ is known,[24] which should facilitate the interpretation of the ESR data.

(24) Willner, H.; Rettig, S.; Trotter, J.; Aubke, F. *Can. J. Chem.* **1991**, 69, 391.

(25) (a) Edwards, A. J.; Jones, G. R.; Sills, R. J. *Chem. Commun.* **1968**, 1527. (b) Edwards, A. J.; Jones, G. R. *J. Chem. Soc. A* **1971**, 2318.

(26) (a) Gillespie, R. J.; Morton, M. J. *Chem. Commun.* **1968**, 1565. (b) Gillespie, R. J.; Morton, M. J. *Inorg. Chem.* **1972**, *11*, 586.

(27) Wilson, W. W.; Thompson, R. C.; Aubke, F. *Inorg. Chem.* **1980**, *19*, 1489.

(28) Cader, M. S. R.; Thompson, R. C.; Aubke, F. *Can. J. Chem.* **1989**, *67*, 1942.

(29) Leung, P. C.; Aubke, F. *Inorg. Chem.* **1987**, *17*, 1765.

(30) Cader, M. S. R.; Thompson, R. C.; Aubke, F. *Chem. Phys. Lett.* **1989**, *164*, 438.

(31) Lee, K. C.; Aubke, F. *Can. J. Chem.* **1977**, *55*, 2473.

(32) Wechsberg, M.; Bulliner, P. A.; Sladky, F. O.; Mews, R.; Bartlett, N. *Inorg. Chem.* **1972**, *11*, 3063.

(33) Lee, K. C.; Aubke, F. *Can. J. Chem.* **1981**, *59*, 2835.

(34) Einstein, F. W. B.; Rao, P. R.; Trotter, J.; Bartlett, N. *J. Chem. Soc. A* **1967**, 478.

(35) Sharpe, A. G. *J. Chem. Soc.* **1949**, 2901.

(36) Nyholm, R. S.; Sharpe, A. G. *J. Chem. Soc.* **1952**, 3579.

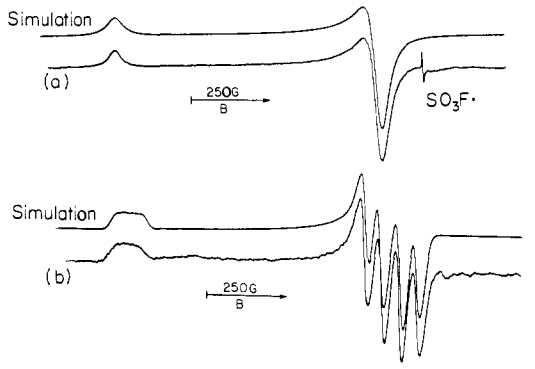

Figure 3. Experimental and simulated ESR spectra of (a) $Au(SO_3F)_{3-x}$ and (b) Au^{2+}(solv) at 103 K. The parameters used for the spectral simulations are listed in Table II.

(iii) In addition, both Raman and IR spectra of $Au(SO_3F)_3$ are reported[11,12] and are easily obtained.

(iv) The solution behavior of $Au(SO_3F)_3$ in HSO_3F is well understood.[12,37] It should be possible to generate Au^{2+}(solv) in this superacidic medium, either by dissolution of partly pyrolyzed $Au(SO_3F)_3$ or reduction of gold(III) by a suitable reagent.

(v) Finally, samples of $Au(SO_3F)_3$, obtained by pyrolysis of $Br_3[Au(SO_3F)_4]$, give extremely broad ESR signals, presumably due to a high concentration of paramagnetic centers in the solid.

The pyrolysis, described in some detail in the Experimental Section, is followed by weight. The very small amounts of volatiles formed are discarded after each temperature increase. The bath temperature is raised from 60 °C to 125 °C. A total weight loss of about 6% and a reduction in sulfur content of about 3%, compared to the calculated value, suggest the loss of a sulfur-containing species. The residue appears to have darkened slightly, and an ESR spectrum is obtained and discussed subsequently. The infrared spectrum of the residue will be discussed later. Interestingly, such samples gave evidence for the presence of trapped $SO_3F^{\bullet}$ radicals in the solid (Figure 3).

Two shorter (~24 h) pyrolysis experiments at 115 and 145 °C, respectively, are undertaken to study the volatile decomposition products formed by IR spectroscopy. In both instances the major volatile products identified by IR spectroscopy are sulfuryl fluoride, SO_2F_2, and silicon(IV) fluoride, SiF_4,[38] with $S_2O_5F_2$ and possibly $S_2O_6F_2$ as minor constituents.

Formation of SO_2F_2 during pyrolysis of fluorosulfates would suggest a rather unusual dissociation with partial formation of a gold(III) sulfate derivative. There is a precedent for this decomposition mode, the pyrolysis of barium and strontium fluorosulfate according to

$$M(SO_3F)_2 \xrightarrow{500\ °C} MSO_4 + SO_2F_2 \qquad (1)$$

$$M = Ba \text{ or } Sr^{39}$$

However, considerably higher temperatures are employed, and the conversion to MSO_4 is reportedly 56–65% within 3 h.[39b]

Alternatively, since $SO_3F^{\bullet}$ radicals react with quartz above 120 °C,[13] interaction with Pyrex is a possible cause for the observation of SO_2F_2 together with SiF_4. Two observations are in support of this explanation: (a) The residue is paramagnetic and ESR active, and, as mentioned, some trapped $SO_3F^{\bullet}$ is occasionally observable in the solid residue. (b) Subsequent treatment of the solid residue with $S_2O_6F_2$ dissolved in HSO_3F for 24 h results in a weight gain and the formation of diamagnetic $Au(SO_3F)_3$. An initial weight loss of 6.3% during pyrolysis is largely offset by an increase of 5.7%, with the small difference likely due to glass attack by $SO_3F^{\bullet}$ radicals. In addition, some of the $SO_3F^{\bullet}$ radicals may have reacted with the sublimed material, found to be ESR-inactive $Au(SO_3F)_3$. In contrast, sublimation of $Au(SO_3F)_3$ at 80 °C in a dynamic vacuum leads to a product that gives an ESR signal.

Another possible, expected volatile product, molecular oxygen, is not detected. No measurable residual pressure is observed when the reactor is cooled to liquid-nitrogen temperature after the completed pyrolysis.

In summary, $Au(SO_3F)_3$ appears to exhibit higher thermal stability than $Br_3[Au(SO_3F)_4]$, judging by the temperatures and times required to achieve partial pyrolysis. Complete pyrolysis leading to well-defined compounds such as $Au(SO_3F)_2$ or $AuSO_3F$ does not appear to occur, as indicated by a DTG (differential thermal gravimetry) experiment (courtesy of Prof. Meyer, Hannover, FRG), which shows gradual decomposition of $Au(SO_3F)_3$ occurring in the temperature range 130–350 °C. Distinct decomposition steps are not detected, some sublimation occurs, and the overall weight loss is slightly above 50%.

The reduction of gold(III) fluorosulfate with gold powder, at a mole ratio of 2.42:1 and at 65 °C with fluorosulfuric acid as solvent, is synthetically more useful. All gold is consumed within 24 h, and a clear brown solution forms that gives an ESR signal. Over a period of 3 days, with the reaction mixture at room temperature, a yellow, diamagnetic precipitate of the composition $Au(SO_3F)_2$ forms and is isolated by filtration. Alternative routes to this compound, its characterization as a mixed-valence compound $Au[Au(SO_3F)_4]$, and its behavior when redissolved in HSO_3F are reported elsewhere.[40] The filtrate solution contains some unreacted $Au(SO_3F)_3$. Its color remains dark brown and gives an ESR signal. The spectrum obtained on a frozen solution is discussed subsequently and is interpreted in terms of a solvated Au^{2+} species. A disproportionation equilibrium of the type

$$2Au^{2+}(solv) + 8HSO_3F \rightleftarrows Au[Au(SO_3F)_4]_{(s)} + 4H_2SO_3F^+ \qquad (2)$$

is suggested, which implies that a high-acidium ion or $H_2SO_3F^+$ concentration will stabilize Au^{2+}(solv), while SO_3F^- ions promote formation of $Au[Au(SO_3F)_4]$.

Support for this view comes from attempts to reduce $Cs[Au(SO_3F)_4]$, which behaves as a base in HSO_3F,[12] with gold powder in HSO_3F as reaction medium. At mole ratios of $Cs[Au(SO_3F)_4]$/Au of 10:1 or 2.9:1, a 60 °C bath temperature subsequently raised to 100 and then to 160 °C, and an overall reaction time of 20 days, unreacted gold powder remains. While some yellow $Au[Au(SO_3F)_4]$ forms, the solution remains yellow throughout. It appears that the initial step, formation of Au^{2+}(solv), is not observable, and $Au[Au(SO_3F)_4]$ becomes the main product.

A relevant precedent for our observation is provided by the behavior of diamagnetic argentic oxide, AgO.[41] Here, disproportionation to Ag^{I}–Ag^{III} in the solid is reversed by dissolution in strong aqueous mineral acids, which allows detection of Ag^{2+}(solv) by ESR.

The mixed-valence $Au[Au(SO_3F)_4]$ also appears to form over several days as a finely divided yellow precipitate when partly pyrolyzed (ESR-active) gold(III) fluorosulfate is dissolved in HSO_3F. However, the small amount of sample used (~80 mg) allows no clear identification of the precipitate. When all volatiles are removed in vacuo, the resulting solid yellow residue gives no ESR signal.

The proposed reductive elimination of the $SO_3F^{\bullet}$ radical on heating is expected to cause changes in the vibrational spectrum of the residues. To demonstrate these changes, IR frequencies of partly pyrolyzed and sublimed $Au(SO_3F)_3$ are listed in Table I and are compared to the corresponding frequencies for $Au(SO_3F)_3$[12a] and $Au[Au(SO_3F)_4]$,[40] both reported previously. All four spectra are recorded as solid films, pressed between AgBr windows.

A comparison considering band positions, shapes, and relative intensities permits a few limited conclusions but does not allow

(37) Cicha, W. V.; Lee, K. C.; Aubke, F. *J. Solution Chem.* **1990**, *19*, 609.
(38) Nakamoto, K. In *Infrared Spectra of Inorganic and Coordination Compounds*; John Wiley, Inc.: New York, NY, 1963; and references therein.
(39) (a) Traube, W.; Hoerenz, J.; Wunderlich, F. *Ber.* **1919**, *52*, 1272. (b) Muetterties, E. L.; Coffman, D. D. *J. Am. Chem. Soc.* **1958**, *80*, 5914.
(40) Willner, H.; Mistry, F.; Hwang, G.; Herring, F. G.; Cader, M. S. R.; Aubke, F. *J. Fluor. Chem.* **1991**, *52*, 13.
(41) McMillan, J. A. *Chem. Rev.* **1962**, *62*, 65 and references therein.

Table I. Infrared Frequencies for $Au(SO_3F)_x$

$Au(SO_3F)_3$ $\bar{\nu}$ (cm^{-1}) int. (PY)	$Au(SO_3F)_3$ $\bar{\nu}$ (cm^{-1}) int. (Su)	$Au(SO_3F)_3$[12a] $\bar{\nu}$ (cm^{-1}) int.	$Au(SO_3F)_3$[40] $\bar{\nu}$ (cm^{-1}) int.
1434 m, sh	1434 m, sh	1442 vs	
1423 m, s	1427 m, s	1425 s, sh	1418 s, sh
1407 s, sh	1405 s, sh		1400 vs
1392 s	1385 s		
1350 m, sh	~1340 w, sh		1369 s
1220 s, sh	1215 ms, sh	1240 s	1232 s
1198 vs	1198 vs	1220 s, sh	1200 vs
1107 m	1112 m	1135 m, s	
			1085 s, b
1052 s, sh	1052 ms, sh	1055 s	1065 m, sh
1037 s	1031 s		1035 ms
			1012 ms
960 m, sh	960 m, sh	960 s, b	962 ms
924 m, br	918 m, br	920 s, sh	931 s
891 s	888 s	895 s, b	870 ms
			836 s
827 ms, sh	830 m, sh	820 s	822 s, sh
809 ms	812 ms		812 s, sh
		682 s	680 ms
664 w	666 mw	670 s, sh	671 m
657 w, sh	655 w, sh		648 m, sh
635 vw, sh		610 w	
586 s	580 s, br	590 s	595 m
576 s		582 s	
541 ms	542 m	550 ms	548
462 w	462 w	460 m	462

Table II. ESR Parameters of Gold(II) and Related Complexes

complex	T (K)	g_1	g_2	g_3	g_{iso}	A_1 (MHz)	A_2 (MHz)	A_3 (MHz)	A_{iso} (MHz)	ref
$Au(SO_3F)_{3-x}$	103	2.093	2.103	2.882	2.359					*a*
Au^{2+} (solv)[b]	103	2.093	2.103	2.890	2.362	145	145	120	133.7	*a*
$[Au[Au(SO_3F)_4]$(solv)	77	2.065	2.234	2.656	2.3183					40
$[Au(mnt)_2]^{2-}$[c]	133	1.9769	2.0051	2.0023	1.9947	117	122	124	121	5
$[Au(mnt)_2]^{2-}$	(d)				2.009				83	8
Au(phthalocyanine)	77				2.065				61	7
$Ag(SO_3F)_2$[e]	77	2.072	2.096	2.407	2.1917					29

[a] This work. [b] For the simulation, the additional parameter Q_{zz} = 46 MHz and the Gaussian line widths $L_1 \approx L_2$ = 20 G and L_3 = 25 G are used. [c] $[Au(mnt)_2]^{2-}$ doped into $[Ni(mnt)_2]^{2-}$. [d] Temperature not stated. [e] In $BrSO_3F$ solution the g_{iso} value differs slightly from the one reported previously.

a detailed vibrational assignment of individual bands. The conclusions are briefly summarized.

(i) Any discrepancies between the tabulated spectra are rather subtle and affect primarily the SO_3F stretching region (1450–800 cm^{-1}) and bands between 600 and 700 cm^{-1}, attributed in part to AuO_4 skeletal stretching vibrations.[12] Even in these regions, partly pyrolyzed and sublimed $Au(SO_3F)_3$ give identical IR spectra.

(ii) Both spectra of the pyrolyzed and sublimed gold(III) fluorosulfate show greater band proliferation than does $Au(SO_3F)_3$. In addition, the highest band frequency, usually attributed to a terminal SO_3F group[42] centered at 1442 cm^{-1} in $Au(SO_3F)_3$,[12] has shifted to lower frequencies on heating and has decreased in intensity.

(iii) Even though the IR spectrum reported for $Au[Au(SO_3F)_4]$ is slightly different, the possible presence of this compound in pyrolyzed and sublimed $Au(SO_3F)_3$ cannot be ruled out.

It is for this reason that the observed weight loss during pyrolysis cannot be related to the generation of Au^{2+} ions in the solid residue. The most reasonable estimate of the Au^{2+} ion concentration is based on the magnetic susceptibility measurements reported here. When the measured value of χ_M^{corr} at 298 K is compared to a calculated value derived from the g_{iso} value obtained by ESR using the spin-only formula, a Au^{2+} content of ~7% is suggested. This value will of course vary from sample to sample depending on the heat treatment. Obviously a considerably lower concentration of Au^{2+} is found in the samples used for ESR studies, in particular in the solvated Au^{2+} species.

In summary, the IR spectra listed in Table I suggest that $Au(SO_3F)_3$, when heated or sublimed in vacuo, undergoes slight structural changes that cause more complex IR spectra. It is tempting to interpret the structural changes as being due to polymerization via bridging fluorosulfate groups after $SO_3F^\bullet$ radicals are eliminated, restoring the distorted square-planar coordination around gold.

All evidence discussed so far is consistent with the partial reductive elimination of $SO_3F^\bullet$ radicals and the possible formation of Au^{2+} defects in the solid residue of the composition $Au(SO_3F)_{3-x}$. Likewise Au^{2+}(solv) is suggested as the initial product when $Au(SO_3F)_3$, dissolved in HSO_3F, is reduced with gold powder before disproportionation to $Au[Au(SO_3F)_4]$ occurs. Interestingly, both ESR spectra obtained on $Au(SO_3F)_{3-x}$ and Au^{2+}(solv), shown in Figure 3 and listed in Table II, together with relevant literature data for other mononuclear Au(II) complexes and for $Ag(SO_3F)_2$, show strong similarities. However, there are two differences: (i) the spectrum obtained on a frozen solution of Au^{2+}(solv) shows well-resolved hyperfine splitting due to ^{197}Au (I = 3/2) and (ii) the hyperfine structure is not resolved for $Au(SO_3F)_{3-x}$, but now a second species is occasionally observed, giving rise to a single line at g = 2.0033. This second species appears to be a minor constituent, and assignment as a $SO_3F^\bullet$ radical is suggested by comparison with published data.

The fluorosulfate radical, best obtained by reversible dissociation of bis(fluorosulfuryl)peroxide, $S_2O_6F_2$,[13] has been studied previously in the condensed phase[43–46] and in HSO_3F solution[46] by

(42) Wilson, W. W.; Aubke, F. *Inorg. Chem.* **1974**, *13*, 326.

(43) Nutkowitz, P. M.; Vincow, G. *J. Am. Chem. Soc.* **1969**, *91*, 5936 and *J. Phys. Chem.* **1975**, *75*, 245.

ESR. All reports agree on a g value of close to 2.011 and a broad, featureless isotropic signal. An asymmetric signal and a g_{iso} value of 1.97267 are observed only in HSO_3F[46] presumably caused by solvate formation of $SO_3F^{\bullet}$ with HSO_3F.

The possible presence of trapped $SO_3F^{\bullet}$ radicals could have affected the magnetic susceptibility measurements reported here, but as seen in Figure 3, the signal due to this species, observed only occasionally in solid samples, is of very low intensity.

The major constituent in the ESR spectrum of the center generated by the pyrolysis of $Au(SO_3F)_3$ is typical of an axial system. The spectrum does not exhibit hyperfine coupling. Simulation of the spectrum was attained using a nearly axial g tensor, $g_1 = 2.103$, $g_2 = 2.093$, and $g_3 = 2.882$, with a Lorentzian line width of 32 G. An axial g tensor does not lead to the correct lineshape in the region around $\simeq 2.1$. Finally, the required use of a Lorentzian rather than a Gaussian lineshape to produce a correct simulation suggests the absence of inhomogeneous broadening.

The ESR spectrum of the center produced by the reduction of $Au(SO_3F)_3$ by Au(s) in HSO_3F recorded from a sample at 100 K exhibits a near-axial spectrum with hyperfine splitting from an $I = 3/2$ nucleus, most probably ^{197}Au. Other possibilities for the interpretation of the hyperfine splitting, such as coupling to two fluorine nuclei, can be ruled out on the basis of the need to include a quadrupole interaction in the simulation. In order to simulate the spectrum on the basis of a nearly axial g tensor and an $I = 3/2$ nucleus, the inclusion of a nuclear quadrupole coupling was necessary. The presence of such an interaction is evident in the sloping intensity pattern in the $g \sim 2.1$ region (high field). The inclusion of a quadrupole coupling constant in the simulation was necessary in order to obtain the correct relative intensities of the lines in the perpendicular manifold of the spectrum. The simulated spectrum with quadrupole coupling absent is enclosed as supplementary material for comparison. The spin Hamiltonian parameters required to simulate the spectrum are $g_1 = 2.096$, $g_2 = 2.103$, $g_3 = 2.890$, $A_1 \simeq A_2 = 145$ MHz, $A_3 = 120$ MHz, and $Q_{zz} = 46$ MHz with anisotropic Gaussian line widths $L_1 \simeq L_2 = 20$ G and $L_3 = 25$ G. It is clear from the above that the g tensor for both centers is the same to within experimental error, suggesting a similar environment for both centers.

The site of Au(III) ion in gold(III) fluorosulfate as seen in detail in Figure 1, is best described as approximately square-planar.[24] However, the two different Au–O bond lengths produce local C_{2v} symmetry at the Au(III) center. There are also very weak interactions, approximately perpendicular to the molecular AuO_4 plane, that are ignored. The orthorhombic nature of the g tensor for the Au(II) center formed by reduction with Au(s) in solution and that formed by pyrolysis of $Au(SO_3F)_3$ suggest that Au(II) occupies in both instances a site very similar to the Au(III) site in gold(III) fluorosulfate. The major difference between the two Au(II) centers is the lack of any observable ^{197}Au hyperfine in the center formed by pyrolysis.

The absence of hyperfine for the center produced by pyrolysis could simply be due to a different distribution of spin density in the SOMO; i.e., less in the 5d orbitals of Au^{2+} in case of Au^{2+}(solv). The near equality of the g tensor components tends to mitigate against this possibility since substantial changes in d-orbital participation in the odd-electron orbital would lead to large changes in the g tensor.

An alternative explanation is based on the possibility that the concentration of Au^{2+} is much higher in the pyrolyzed sample, leading to dipolar broadening washing out the hyperfine splitting. Because the spectra for both samples of roughly the same mass were recorded under identical conditions of modulation amplitude and power, it seems unlikely that this explanation is correct, unless one assumes an additional reduction of Au^{2+}(solv) concentration has occurred due to the disproportionation equilibrium 2, resulting in the formation of diamagnetic $Au[Au(SO_3F)_4]$.

If the absence of the Au(II) hyperfine in the pyrolyzed sample is not due to changes in spin density or to Au(II) concentrations, it may be due to motional averaging of the hyperfine coupling in the solid-state sample. We note that the line width used in the simulation of the signal from the pyrolyzed sample is ca. 3/2 times the line width of the observed hyperfine in the Au^{2+}(solv) sample, so that hyperfine coupling of ca. 50 g should be observed for the pyrolyzed sample. The nature of the motional averaging is open to speculation.

There is another common link between the two Au(II) centers generated either in the solid state or in solution. In both instances unreduced gold(III) is present. With gold(III) fluorosulfate dimeric in the solid state[24] and very probably also in HSO_3F solution as well,[37] it becomes likely that the Au(II) center is found in an oligomeric structure, where the additional Au(III) will strongly influence the structure toward square-planar for both gold centers. Interestingly, when diamagnetic $Au[Au(SO_3F)_4]$ is redissolved in HSO_3F or Au^{2+}(solv) is generated in HSO_3F using an exact stoichiometric ratio of 2 mol $Au(SO_3F)_3$ to 1 mol Au, a very asymmetrically coordinated gold(II) species forms in solution with three different g tensors, but a similar g_{iso} of 2.318 and the presence of a monomeric Au(II) species is suggested.[40] Addition of $Au(SO_3F)_3$ to this solution restores the nearly axially symmetrical spectrum observed here in solution of HSO_3F.

Summary and Conclusions

The difference between Au^{2+} species reported here and the complexes reported previously[1,2,5,7-9] and examples listed in Table II is due to the solvent or to the anion used to stabilize the gold(II) cation, in our case the acid HSO_3F, and its selfionization ion SO_3F^-. The former is one of the strongest protonic acids, which has been used in the past to stabilize unusual cations,[48] while the latter is one of the least basic anions.[49] Neither is readily reduced nor capable of acting as a π-acceptor, unlike the ligands used previously.[1,2,5,7-9]

The same two groups of ligands and solvents are also found to form complexes with Ag^{2+}. So far only the fluoride,[50] the fluorosulfate,[29] and the related trifluoromethylsulfate anions[51] are capable of stabilizing Ag^{2+} in binary compounds or ternary complexes, with similar magnetic properties and ESR parameters[29] as reported here, considering the differences in the spin-orbital coupling constant of Ag^{2+} ($\sim$1800 cm^{-1}) and Au^{2+} ($\sim$5000 cm^{-1})[47] and the higher concentration of paramagnetic centers, which in the case of $Ag(SO_3F)_2$ generates a very broad single-line spectrum. However, for a frozen solution of the compound in $BrSO_3F$ a Ag^{2+} species in a similar spectrum as in $Au(SO_3F)_{3-x}$ is observed,[29] typical for an axial system. The magnetic moment μ_{eff} of 1.90 μ_B obtained for $Ag(SO_3F)_2$ by using the spin-only formula compares well with a value of 1.92 μ_B from bulk magnetic susceptibility measurements. A spin-only μ_{eff} value for gold of 2.05 μ_B based on $g_{iso} = 2.360$ appears to be eminently reasonable for this cation. On the other hand, a large number of complexes with π-acceptor ligands are reported for silver(II),[52] which resemble in their molecular structures and ESR characteristics those of the previously reported gold(II) complexes.[1,2,5-9]

The very much reduced stability of Au^{2+} compared to Ag^{2+} and its pronounced tendency to disproportionate to Au(I) and Au(III) are reflected in the fact that no previous reports on Au^{2+} exist and that we have been unable to obtain pure, paramagnetic $Au(SO_3F)_2$. Reasons for this discrepancy in the chemistry of Ag^{2+}

(44) Stewart, R. A.; Fujiwara, S.; Aubke, F. *J. Chem. Phys.* **1968**, *48*, 5524.
(45) Neumayr, F.; Vanderkooi, N. *Inorg. Chem.* **1965**, *4*, 1234.
(46) Cicha, W. V.; Herring, F. G.; Aubke, F. *Can. J. Chem.* **1990**, *68*, 102.
(47) Dunn, T. M. *Faraday Trans.* **1961**, *57*, 1441.
(48) (a) Thompson, R. C. In *Inorganic Sulphur Chemistry*; Nickless, G., Ed.; Elsevier: Amsterdam, The Netherlands, 1968. (b) Gillespie, R. J. *Acc. Chem. Res.* **1968**, *1*, 202. (c) Olah, G.; Prakash, G. K. S.; Sommer, J. *Superacids*; Wiley: New York, NY, 1985.
(49) Mallela, S. P.; Yap, S.; Sams, J. R.; Aubke, F. *Inorg. Chem.* **1986**, *25*, 4327.
(50) Müller, B. J. *Angew. Chem., Int. Ed. Engl.* **1987**, *26*, 861.
(51) Leung, P. C.; Lee, K. C.; Aubke, F. *Can. J. Chem.* **1979**, *57*, 326.
(52) (a) Po, N. H. *Coord. Chem. Rev.* **1976**, *20*, 171. (b) Lancashire, R. J. In *Comprehensive Coordination Chemistry*; Wilkinson, G., Ed.; Pergamon Press: Oxford, U.K., 1987; Vol. 5, p 775.

and Au^{2+} have been discussed elsewhere.[1,2]

Acknowledgment. Financial support by the Natural Sciences and Engineering Council of Canada (NSERC), Deutsche Forschungsgemeinschaft (DFG), and North Atlantic Treaty Organization (NATO) for a collaborative research grant to H.W. and F.A. is gratefully acknowledged.

Registry No. Au, 7440-57-5; $Br_3[Au(SO_3F)_4]$, 72030-07-0; $Au(SO_3F)_3$, 36735-27-0; Au^{2+}, 15456-07-2; SO_2F_2, 2699-79-8; SiF_4, 7783-61-1.

Supplementary Material Available: Experimental and simulated ESR spectra, the latter with and without quadrupole coupling (2 pages). Ordering information is given on any current masthead page.

A New Model for Dioxygen Binding in Hemocyanin. Synthesis, Characterization, and Molecular Structure of the μ-η^2:η^2 Peroxo Dinuclear Copper(II) Complexes, $[Cu(HB(3,5\text{-}R_2pz)_3)]_2(O_2)$ (R = *i*-Pr and Ph)

Nobumasa Kitajima,*,† Kiyoshi Fujisawa,† Chisato Fujimoto,† Yoshihiko Moro-oka,*,† Shinji Hashimoto,‡ Teizo Kitagawa,*,‡ Koshiro Toriumi,‡ Kazuyuki Tatsumi,*,§ and Akira Nakamura§

Contribution from the Research Laboratory of Resources Utilization, Tokyo Institute of Technology, 4259 Nagatsuta, Midori-ku, Yokohama 227, Japan, the Institute for Molecular Science, Okazaki National Institutes, Myodaiji 444, Okazaki, Japan, and the Department of Macromolecular Science, Osaka University, Toyonaka, Osaka 560, Japan.
Received May 20, 1991

Abstract: The synthesis and characterization of μ-η^2:η^2 peroxo dinuclear copper(II) complexes which show many similarities to oxyhemocyanin (or oxytyrosinase) in their physicochemical properties are presented. The low-temperature reaction of a di-μ-hydroxo copper(II) complex $[Cu(HB(3,5\text{-}i\text{-}Pr_2pz)_3)]_2(OH)_2$ (**8**) with H_2O_2 gave a μ-peroxo complex $[Cu(HB(3,5\text{-}i\text{-}Pr_2pz)_3)]_2(O_2)$ (**6**). Complex **6** was also prepared by dioxygen addition to a copper(I) complex $Cu(HB(3,5\text{-}i\text{-}Pr_2pz)_3)$ (**9**). The preparation of an analogous peroxo complex $[Cu(HB(3,5\text{-}Ph_2pz)_3)]_2(O_2)$ (**7**) was accomplished by the similar dioxygen treatment of a copper(I) acetone adduct $Cu(Me_2CO)(HB(3,5\text{-}Ph_2pz)_3)$ (**10**). The reaction of **6** with CO or PPh_3 causes release of dioxygen, resulting in formation of the corresponding copper(I) adduct, $Cu(CO)(HB(3,5\text{-}i\text{-}Pr_2pz)_3)$ (**11**) or $Cu(PPh_3)(HB(3,5\text{-}i\text{-}Pr_2pz)_3)$ (**12**). Crystallography was performed for **6**-6(CH_2Cl_2), **8**-1.5(CH_2Cl_2), and **11**. Compound **6**-6(CH_2Cl_2) crystallizes in the monoclinic space group $C2/c$ with a = 26.36 (2) Å, b = 13.290 (4) Å, c = 29.29 (2) Å, β = 114.59 (6)°, V = 7915 (9) Å^3, and Z = 4. The refinement converged with the final R (R_w) value, 0.101 (0.148), for 3003 reflections with $F \geq 3\sigma(F_o)$. Compound **8**-1.5(CH_2Cl_2) crystallizes in the triclinic space group $P\bar{1}$ with a = 16.466 (4) Å, b = 16.904 (5) Å, c = 14.077 (3) Å, α = 112.92 (2)°, β = 99.21 (2)°, γ = 90.76 (2)°, V = 3550 (2) Å^3, Z = 2, and the final R (R_w) factor, 0.083 (0.105), for 7226 reflections with $F \geq 3\sigma(F_o)$. Compound **11** crystallizes in the monoclinic space group, $P2_1/a$ with a = 16.595 (4) Å, b = 19.154 (4) Å, c = 10.359 (2) Å, β = 106.65 (2)°, V = 3155 (1) Å^3, Z = 4, and the final R (R_w) value 0.083 (0.074) for 5356 reflections with $F \geq 3\sigma(F_o)$. The X-ray analysis of **6**-6(CH_2Cl_2) definitely established the μ-η^2:η^2 coordination structure of the peroxide ion for the first time. This unusual side-on structure is entirely novel for a d-block element transition-metal–dioxygen complex. Both **6** and **7** show remarkable characteristics which are very similar to those known for oxyhemocyanin and oxytyrosinase. Complex **6**: diamagnetic; ν(O–O), 741 cm^{-1}; UV–vis, 349 nm (ϵ, 21 000), 551 nm (ϵ, 790); Cu–Cu, 3.56 Å. Complex **7**: diamagnetic, ν(O–O), 759 cm^{-1}; UV–vis, 355 nm (ϵ, 18 000), 542 nm (ϵ, 1040). These properties are all consistent with those of an analogous complex, $[Cu(HB(3,5\text{-}Me_2pz)_3)]_2(O_2)$ (**5**), of which the characterization and reactivities were reported already (Kitajima, N., et al. *J. Am. Chem. Soc.* **1990**, *112*, 6402; **1991**, *113*, 5664). The magnetic and spectroscopic features of **5**–**7** and their biological relevance are discussed in detail. Furthermore, simple interpretation of the electronic state of the $N_3Cu(O_2^{2-})CuN_3$ chromophore is provided based on extended Hückel MO calculations. The close resemblance between the properties of μ-η^2:η^2 peroxo complexes **5**–**7** and oxyhemocyanin led us to propose a new model for dioxygen binding in hemocyanin; dioxygen is simply bound between the two copper ions in the μ-η^2:η^2 mode. With this structural model; the existence of an endogenous bridging ligand, which has been generally supposed to account for the diamagnetism of oxyhemocyanin, is no longer necessary.

Introduction

Hemocyanin (Hc) is a ubiquitous oxygen transport protein for invertebrates: arthropods and molluscs.[1-3] Hc contains a dinuclear copper site with a Cu–Cu separation of ca. 3.6 Å.[4,5] Dioxygen is known to bind to this site as a peroxide ion in a symmetric coordination mode.[6-8] Accordingly, the valence change of the copper ions is interpreted in terms of a two-electron oxidation: Cu(I,I) in deoxy-Hc and Cu(II,II) in oxy-Hc. A striking feature of oxy-Hc is its diamagnetism due to the strong antiferromagnetic coupling between the two copper(II) ions ($-2J > 600$ cm^{-1}).[9,10] Furthermore, instead of the weak d–d transitions at

† Tokyo Institute of Technology.
‡ Institute of Molecular Science.
§ Osaka University.

(1) *Structure and Function of Hemocyanin*; Bannister, J. V., Ed.; Springer-Verlag: Berlin, Heidelberg, New York 1977.
(2) Solomon, E. I.; Penfield, K. W.; Wilcox, D. E. *Struct. Bonding (Berlin)* **1983**, *53*, 1-57.
(3) Solomon, E. I. *Metal Clusters in Proteins*; Que, L., Jr., Ed.; ACS Symposium Series 372, American Chemical Society: Washington, D.C., 1988; pp 116-150.
(4) (a) Gaykema, W. P. J.; Hol, W. G. J.; Vereijken, J. M.; Soeter, N. M.; Bak, H. J.; Beintema, J. J. *Nature* **1984**, *309*, 23-29. (b) Gaykema, W. P. J.; Volbeda, A.; Hol, W. G. J. *J. Mol. Biol.* **1985**, *187*, 255-275.
(5) (a) Volbeda, A.; Hol, W. G. J. *J. Mol. Biol.* **1989**, *206*, 531-546. (b) Volbeda, A.; Hol, W. G. J. *J. Mol. Biol.* **1989**, *209*, 249-279.

0002-7863/92/1514-1277$03.00/0